Vol. 85 (1994) ACTA PHYSICA POLONICA A No. 1

Proceedings of the European Conference "Physics of Magnetism 93", Poznań 1993

CATION DISTRIBUTION IN $Fe_{3(1-\delta)}O_4$ AND LOW LEVEL DOPED $Fe_{3-x}M_xO_4$, M = Ti, Zn, Al

Z. KĄKOL, A. KOZŁOWSKI

Department of Solid State Physics, Faculty of Physics and Nuclear Techniques
University of Mining and Metallurgy, Al. Mickiewicza 30, 30-059 Kraków, Poland

J. SABOL, P. METCALF AND J.M. HONIG

Department of Chemistry, Purdue University, West Lafayette, IN 47907, USA

Systematic magnetic saturation moment and electrical resistivity measurements of the $Fe_{3(1-\delta)}O_4$ and $Fe_{3-x}M_xO_4$ (M = Ti, Zn, Al) are presented. Cation distributions for low level doping are proposed and compositional dependencies of the Verwey transition temperature are determined. The latter show striking similarities in their dependence on cation vacancies and dopant concentration for any extraneous cations. These data are the basis for the analysis of the correlation between the presented cations distributions and the Verwey transition.

PACS numbers: 72.80.Ga, 75.30.Cr, 7550.Gg

1. Introduction

The Verwey transition in magnetite has been the subject of intensive studies for the last fifty years (for representative topical reviews, the reader is referred to references [1–3]). Despite such a tremendous interest many features of this phase transition are still not completely understood. Above the transition temperature T_V magnetite crystallizes in the inverse cubic spinel structure, where Fe^{2+} cations reside solely in the octahedral sublattice, while Fe^{3+} are present on both sublattices [4]. Correlated electrons from Fe^{2+} resonating between octahedral sites are responsible for the high electrical conduction of this material. At the Verwey transition, there is the change of symmetry from cubic to monoclinic [5], and the resonating electrons freeze out causing the substantial rise in resistivity. It was reported recently [6–9] that both T_V and the character of the transition is strongly affected by oxygen nonstoichiometry and by partial substitution of Fe with Zn, Ti or Al. A systematic investigation performed on $Fe_{3(1-\delta)}O_4$, and/or $Fe_{3-x}M_xO_4$ (where M = Zn or Ti) revealed that for $3\delta = x > 0.012$ the transition changes from first to second (or higher) order. Moreover, the transition temperature decreases linearly with increasing cation vacancy density or metal substitution, with

the universal correspondence $3\delta \equiv x$ that holds for nonstoichiometric magnetite, zinc ferrite and titanomagnetite. A cation redistribution and the change of Fe^{2+} to Fe^{3+} ratio takes place as a result of doping or oxidation process. In order to understand the mechanism of the transition, this cation distribution must be precisely determined. We show, by means of saturation magnetic moment measurements, that for nonstoichiometric as well as Ti and Zn substituted magnetite, Fe^{2+} ions reside only on octahedral positions, while Al doping forces Fe^{2+} to enter both sublattices. Consequences of this fact are discussed below.

2. Experiment

Single crystals of $Fe_{3-x}M_xO_4$ ($0 \leq x < 0.06$) with M = Al, Ti, Zn were grown in a CO–CO_2 atmosphere in a skull melter by techniques detailed elsewhere [10–12]. Using this procedure, it was possible to maintain a given charge above its melting point for several hours, and through convective stirring to optimize the uniform distribution of M in the host material. The M distribution and actual composition were checked for each crystal using a microprobe electron analyzer. Single crystals were then reannealed under the appropriate CO–CO_2 gas mixture [13] using an oxygen transfer cell [14] to monitor the oxygen fugacity. Annealing conditions were selected to obtain a series of nonstoichiometric magnetite $Fe_{3(1-\delta)}O_4$ specimens, and to attain the ideal, stoichiometric 4 : 3 oxygen-to-cation ratio for each specimen with $x > 0$ [9, 15, 16]. The uncertainty in the oxygen stoichiometry was estimated to be 4 ± 0.0001. Anneals were performed in the temperature range 1200–1400°C for 48 h. The material was then rapidly quenched and trimmed to obtain specimens of uniform oxygen and M composition. Each sample was subsequently ground into a small sphere of 1.5–2 mm for magnetization measurements, whereas bars of approximately 2 mm × 2 mm × 8 mm were prepared for resistivity measurements. Since the sample volume was only a fraction of the original crystal, each specimen was cut open upon completion of the measurements and the composition was checked using the microprobe analyzer. The error in x was estimated to be smaller than $\Delta x = \pm 0.0010$ for first order samples ($x < 0.012$) and from ± 0.0015 up to ± 0.0025 for second order samples.

Saturation measurements were performed with a vibrating sample magnetometer at the temperature 4.2 K and in the magnetic field of 15 kOe applied along magnetic easy direction. The unique easy axis, for the low temperature phase, was established through the appropriate magnetic field-cooling procedure, described in details elsewhere [17].

Dc resistivity measurements were performed from room temperature to liquid helium on both cooling and heating cycles. Four-probe leads were soldered ultrasonically in conventional fashion. The resistivity measurements included provision for current reversal.

3. Results

The dependence on M concentration and nonstoichiometry parameter δ of the saturation magnetic moment at 4.2 K is presented in Fig. 1. The four lines

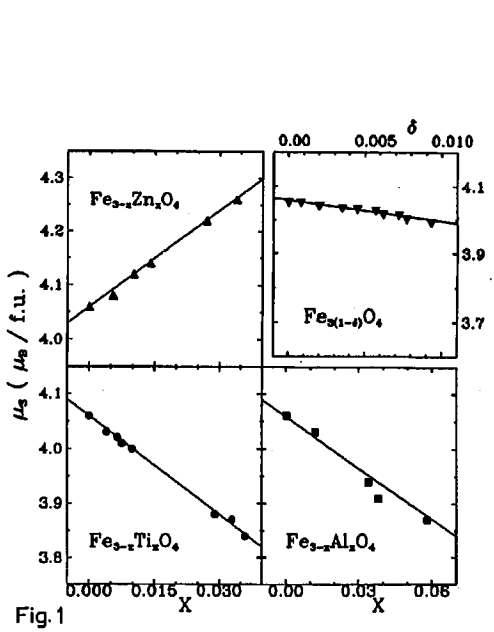

Fig. 1

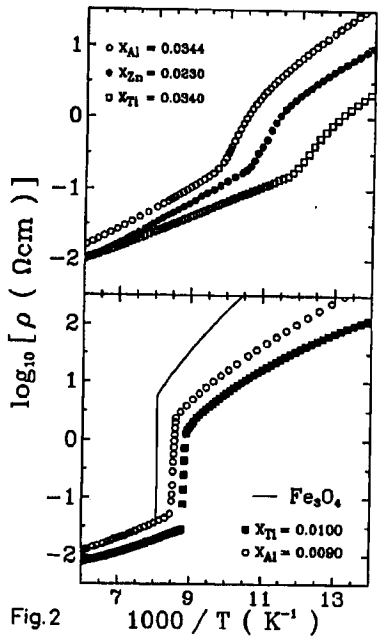

Fig. 2

Fig. 1. Saturation magnetic moment of $Fe_{3(1-\delta)}O_4$ and $Fe_{3-x}M_xO_4$ (M = Zn, Ti and Al) at 4.2 K

Fig. 2. Variation of resistivity ρ with temperature for selected samples of $Fe_{3(1-\delta)}O_4$ and $Fe_{3-x}M_xO_4$ (M = Zn, Ti and Al) in the vicinity of the Verwey transition.

shown in Fig. 1 represent calculated values for the most reasonable cation distribution based on high doping concentration [17–20]. Experimental data fit very well with theoretical lines. The following cation distributions emerge from these data:

(i) $(Fe^{3+})[Fe^{2+}_{1-9\delta}Fe^{3+}_{1+6\delta}]O_4$,

(ii) $(Fe^{3+}_{1-x}Zn^{2+}_x)[Fe^{2+}_{1-x}Fe^{3+}_{1+x}]O_4$,

(iii) $(Fe^{3+})[Fe^{2+}_{1+x}Fe^{3+}_{1-2x}Ti^{4+}_x]O_4$ and

(iv) $(Fe^{2+}_{0.385x}Fe^{3+}_{1-0.5x}Al^{3+}_{0.115x})[Fe^{2+}_{1-0.385x}Fe^{3+}_{1-0.5x}Al^{3+}_{0.885x}]O_4$,

where () parentheses denotes tetrahedral (t) positions, and [ ] brackets denote octahedral sublattice (o) positions. These distributions indicate that Zn enters exclusively tetrahedral sublattice, Ti exclusively octahedral sublattice, whereas Al enters both; in nonstoichiometric magnetite iron vacancies are created only on octahedral positions. It is worth noting here that the best fit of experimental data for Al doped magnetite differs slightly from that proposed by Dehe et al. [20] and shown above, but the difference remained still within the overall experimental error.

In Fig. 2 representative $\log \rho$ vs. $1/T$ plots are presented for selected specimens in the vicinity of the transition. It is evident that the transition changes its character from first (lower plot) to higher order (upper plot). Moreover, both the transition temperature T_V and resistivity jump change with x and δ.

4. Discussion

M doping and vacancy creation have a profound effect on Fe^{2+} density, i.e. carrier concentration. Due to electroneutrality constraints, in zinc ferrite and nonstoichiometric magnetite some of Fe^{2+} ions are converted to Fe^{3+} ions (carriers are removed from the system), or as in $Fe_{3-x}Ti_xO_4$ some of the Fe^{3+} ions are reduced to Fe^{2+} ions (generating additional carriers). For both $Fe_{3(1-\delta)}O_4$ and $Fe_{3-x}M_xO_4$ with M = Zn or Ti, Fe^{2+} cations still reside on octahedral sublattice, as in pure magnetite. Aluminum doped Fe_3O_4 is unique in the sense that although the number of Fe^{2+} does not change, these ions are present also on (t) sites.

As seen in Fig. 3, the universal correspondence of transition temperature versus $3\delta \equiv x$ which exists for nonstoichiometric magnetite, zinc ferrite and titanomagnetite does not hold for $Fe_{3-x}Al_xO_4$. This can be rationalized by the analysis of the dominant interactions in magnetite. It is accepted that strong electron correlations resulting from (o–o) nearest neighbour Coulomb interactions must be taken into account when explaining the Verwey transition. These interactions determine the electronic short range order. However, an additional interaction must be considered to stabilize the long range ordered state: for example the next-nearest neighbour (t–o) interactions can be included [21]. The later is supported by the observation of anomalous T_V vs. x_{Al} changes. In this system the new (t–o) interactions between Fe^{2+} cations are introduced which may strongly affect long range order and, consequently, the transition temperature.

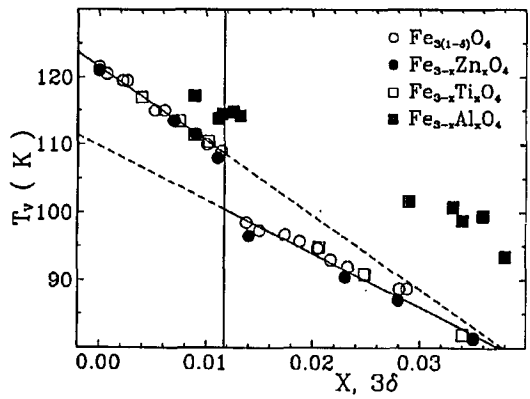

Fig. 3. Dependence of the Verwey transition temperature T_V on composition or on oxygen stoichiometry.

The conjecture of the importance of the (t–o) interactions additionally follows from the observation that an analysis based only on carrier densities of oc-

tahedral sites is not sufficient to account for experimentally observed T_V vs. composition dependence [9].

References

[1] N. Tsuda, K. Nasu, A. Yanase, K. Siratori, *Electronic Conduction in Oxides*, Springer Verlag, Berlin 1991, Ch. 4.8 and references therein.

[2] J.M. Honig, *J. Solid State Chem.* **45**, 1 (1982).

[3] Z. Kąkol, *J. Solid State Chem.* **88**, 104 (1990).

[4] W.C. Hamilton, *Phys. Rev.* **110**, 1050 (1958).

[5] G. Shirane, S. Chikazumi, J. Akimitsu, Y. Fujii, *J. Phys. Soc. Jpn.* **39**, 949 (1975).

[6] P. Wang, Z. Kąkol, M. Wittenauer, J.M. Honig, *Phys. Rev. B* **42**, 4553 (1990).

[7] J.P. Shepherd, J.W. Koenitzer, R. Aragon, J. Spałek, J.M. Honig, *Phys. Rev. B* **43**, 8461 (1991).

[8] Z. Kąkol, J. Sabol, J. Stickler, J.M. Honig, *Phys. Rev. B* **46**, 1975 (1992).

[9] A. Kozłowski, P. Metcalf, in preparation.

[10] H.R. Harrison, R. Aragón, *Mater. Res. Bull.* **13**, 1097 (1978).

[11] R. Aragon, Ph.D. Thesis, Purdue University, 1979.

[12] P. Wang, M.A. Wittenauer, D.J. Buttrey, Q.W. Choi, P. Metcalf, Z. Kąkol, J.M. Honig, *J. Cryst. Growth* **104**, 285 (1990).

[13] R. Aragon, D.J. Buttrey, J.P. Shepherd, J.M. Honig, *Phys. Rev. B* **31**, 430 (1985).

[14] J.P. Shepherd, C.J. Sandberg, *Rev. Sci. Instrum.* **55**, 1696 (1984).

[15] R. Aragon, R.H. McCallister, *Phys. Chem. Minerals* **8**, 112 (1982).

[16] P. Wang, Q.W. Choi, J.M. Honig, *Z. Anorg. Allg. Chem.* **550**, 91 (1987).

[17] Z. Kąkol, J.M. Honig, *Phys. Rev. B* **40**, 9090 (1989).

[18] Z. Kąkol, J. Sabol, J.M. Honig, *Phys. Rev. B* **43**, 649 (1991).

[19] J.W. Koenitzer, Ph.D. Thesis, Purdue University, 1992.

[20] G. Dehe, B. Seidel, K. Melzer, C. Michalk, *Phys. Status Solidi A* **31**, 439 (1975).

[21] D. Ihle, B. Lorenz, *Philos Mag. B* **42**, 337 (1980).